RSC Advances

ROYAL SOCIETY
OF CHEMISTRY

www.rsc.org/advances

Journal Name RSCPublishing

ARTICLE

Adventures in Corrole Features by Electrospray Ionization Mass Spectrometry Studies

Cite this: DOI: 10.1039/x0xx00000x

Received 00th January 2014,
Accepted 00th January 2014

DOI: 10.1039/x0xx00000x

www.rsc.org/

Bernardo A. Iglesias,* Joana F. B. Barata, Catarina I. V. Ramos, M. Graça Santana-Marques, M. Graça P. M. S. Neves and José A. S. Cavaleiro*

In this short review the importance of electrospray mass spectrometry in corrole chemistry is highlighted. ESI-MS and ESI-MS/MS are depicted as important tools for the identification and characterization of novel corrole derivatives. Metallocorrole chemistry and differentiation of corrole isomers *via* ESI-MS/MS and/or TWIM-MS were chosen as two focal points.

Introduction

The pioneering studies developed initially by Fisher[1] and lately by Woodward[2] and other groups on porphyrins and by Johnson and Kay[3,4] on corroles were responsible by the exciting chemistry associated to these two types of macrocycles.

Today, the importance of porphyrin derivatives is not only limited to their central role in vital functions, like respiration and photosynthesis, but also to their applications in several fields such as medicine,[5] catalysis[6] and new electronic materials.[7]

Although corrole chemistry is still far from being as well explored as porphyrin chemistry, corroles are now considered an independent group of macrocycles within the larger family of tetrapyrrolic compounds. This is mainly due to the advances made on the synthetic methodologies of these macrocycles,[8-13] in special to the huge effort devoted to their functionalization,[14] to obtain high value corroles with potential applications in several fields.

In fact, the interest on these compounds has increased significantly over the past decade, and currently, the popularity of corroles is, in some cases, approaching that of porphyrins.[15-26]

Corroles have properties which are different from those of their porphyrin counterparts. These properties are due to their corrin-like structural carbon skeleton, which is the cause of their lower symmetry,[27] increased ring tension, due to the direct β-β pyrrole connection, tautomeric isomerism of the core[28] and coordination with trivalent metal cations.[29] In terms of electronic structure, corroles are aromatic macrocycles with an 18π-electron conjugated system similar to that of porphyrins,[30] which is able to coordinate effectively metal ions in high oxidation states. Thus the smaller trianionic corrolato ligand has a greater ability to stabilize metal centres in higher oxidation states and open-shell electron configurations, than the larger dianionic porphyrinato ligand.[31]

The establishment of efficient synthetic routes for tetrapyrrolic macrocycles has been an important objective over the years. Since the first synthesis reported by Rothemund in 1935[32] concerning the non-natural *meso*-substituted β-free porphyrin **1** (Fig. 1), a large number of synthetic methodologies have been reported. This progress in porphyrin chemistry had not a parallel situation in the case of corroles until recently. The real boost in the chemistry of these compounds started in 1999 with the development, by Gross[9] and Paolesse,[10] of simple and efficient synthetic methodologies leading to *meso*-substituted corroles **2** (Fig. 1). Based on these synthetic approaches, new progresses were made by other research groups. In particular, Gryko´s group was able to refine the experimental conditions giving access to *meso*-substituted A_3- and *trans*-A_2B-corroles.[11-13] Other synthetic methodologies have been reported introducing different approaches such as microwave irradiation,[33] heterogeneous acid catalysts[34] and ionic liquid as solvent.[35]

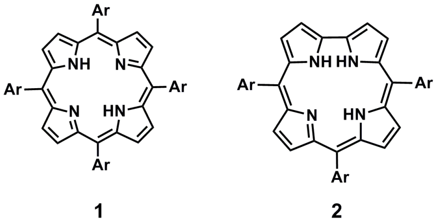

Fig. 1 General structures of *meso*-tetra(aryl)porphyrins **1** and *meso*-tri(aryl)corroles **2**.

The development of synthetic pathways leading to *meso*-tri(aryl)corroles has been accompanied by a considerable effort in the establishment of strategies for their functionalization and several conventional procedures are now well established. These involve, for example, halogenation,[36-42] sulfonation/chlorosulfonation,[43-46] nitration/amination,[46,47-53] nucleophilic aromatic substitution,[17,53,54] cycloaddition[55-60] and metal catalysed reactions.[61-72] Concerning porphyrins it can be said, with some certainty, that virtually any kind of substituted porphyrin can now be synthesized, just by "*one-pot*" reactions, or by multiple synthetic steps depending on the substituent.

Several techniques contributed to the structural characterization of these macrocycles, namely NMR, XRD, absorption and emission spectroscopy, cyclic voltammetry and mass spectrometry. In particular, mass spectrometry has played an important role as a versatile tool in the characterization of such compounds.

Tetrapyrrolic macrocycles, in special the porphyrins, have been studied by mass spectrometry using different ionization techniques. Initially, electron ionization (EI) was used, but unwanted gas-phase decompositions[73] led to the use of alternative ionization techniques. Nevertheless an important diagnostic cleavage of the porphyrin macrocycle was reported under electron impact.[74] Chemical ionization (CI) was also used, and for some porphyrins and metalloporphyrins, formation of the corresponding porphyrinogens was observed.[75,76] This feature led to the development of a method for pyrrole sequencing, by CI.[77] Field desorption (FD) was used to characterize porphyrins from mixtures of natural sources as early as 1975[78]; a similar procedure was applied for the characterization of metallophthalocyanins.[79] FD and other ionization techniques were also used to analyse the oxidation products of corroles.[80] Desorption ionization techniques, using a liquid matrix, such as fast atom bombardment (FAB) and liquid secondary ion mass spectrometry (LSIMS) were also used, for instance to characterize metallated phthalocyanines,[81] and porphyrins,[82,83] and also free base chlorins and bacterichlorins.[84] More recently, matrix-assisted laser desorption/ionization (MALDI) and electrospray ionization (ESI) have been increasingly used in the characterization of tetrapyrrolic macrocycles. MALDI has been applied to study porphyrins, azaporphyins, phthalocyanines, multiporphyrin arrays,[85,86] products from the photolysis of chlorins and bacteriochlorins,[87,88] and corrole derivatives.[89] ESI has been used in the case of free base and metallated, neutral and cationic, porphyrins90-99 and also in the study of the interactions of cationic porphyrins with nucleotides.[100-102]

Besides ESI, other less common atmospheric pressure ionization techniques, such as atmospheric pressure photoionization (APPI) and atmospheric pressure chemical ionization (APCI), have been used, namely for metallochlorins,[88] metalloporphyrins[103] and corrole derivatives.[80,104]

Notwithstanding its advantages and in contrast with the extensive use of MS techniques in porphyrin chemistry, the role of MS in corrole characterization is still very limited. Most of the reported papers on this topic describe the use of ESI-MS in the characterization of corroles, especially via accurate mass measurements,[58,89,105-115] although a few studies of their gas-phase chemistry, using this technique, have been published.[54,80,104,116-121] These included the structural differentiation of corrole isomers by techniques such as TWIM-MS (travelling wave ion mobility mass spectrometry)[118-120] and the investigation of their gas-phase coordination chemistry.[117] MALDI has been less used, as for instance in the radical induced fragmentation of amino acid ester corroles,[89] along with ESI, and in the corrole titrations with fluoride and cyanide anions.[25,26]

In this review the use of ESI-MS in the analysis of corrole derivatives will be highlighted, mainly their gas-phase coordination chemistry and the differentiation of isomers *via* ESI-MS^n (n>2) and ESI-TWIM-MS. Relevant related studies with porphyrins will be also reported on a comparison basis.

Mass spectrometry techniques used to study tetrapyrrolic macrocycles

The first studies on tetrapyrrolic macrocycles by mass spectrometry used ionization techniques such as electron ionization (EI) and chemical ionization (CI). Although both techniques are still used, they can only be applied to the analysis of volatile, thermally stable compounds, because the first step of these ionization processes is the vaporization of the analyte achieved by heating. In the case of EI, once in the gas-phase, the neutral analyte, M, interacts with a homogeneous beam of electrons (typically at 70 electron volts energy), causing its ionization, usually as radical cations $M^{+\bullet}$, and fragmentation. The later usually follows predictable pathways giving rise to fragment ions which convey structural information about the analyte. In the case of CI, a reagent gas (for instance, ammonia or methane) is partially ionized by an electron beam and then reacts with the unionized reagent gas, usually, to form protonated reagent gas molecules. The ionization of the vaporized analyte is due to proton transfer from the reagent, with formation of the protonated analyte molecules, $[M+H]^+$, and is therefore a much lower energy process than EI, so that fragmentation is greatly reduced. As both EI and CI require volatilization of the analyte, these techniques can only be used for compounds with molecular masses up to, and around, 500 Da.

The analysis of polar and non-volatile analytes was initially achieved by FD. In this technique, a high-potential electric field is applied to an emitter (generally a filament), to which the analyte is directly applied, as a thin film or as small crystals, leading to the formation of ionized molecules of the analyte. The process produces radical cations $M^{+\cdot}$ and less often, protonated molecules $[M+H]^+$, both with low internal energies , thus the mass spectra produced by FD show few fragment ions or no fragment ions at all. FD has largely been supplanted by newer ionization techniques, namely, FAB, LSIMS, ESI, MALDI and others.

In the case of FAB and LSIMS, the analyte is mixed with a non-volatile matrix and then is bombarded, under vacuum, in the case of FAB with a high energy beam of atoms (Ar, Xe) and in the case of LSIMS by accelerated primary ions (Ar^+, Xe^+, Cs^+). Common matrices include glycerol, thioglycerol and 3-nitrobenzyl alcohol. With the introduction of FAB and LSIMS less volatile and more labile tetrapyrrolic compounds could be analysed, which include compounds with molecular masses up to 6000 Da. Depending on the matrix and on the analyte either $M^{+\cdot}$ or $[M+H]^+$ ions, or both, can be formed by FAB and LSIMS.

MALDI is a two-step ionization process, in which a laser beam is used to desorb the analyte, co-crystalized with a matrix. The matrix absorbs radiation at the laser wavelength, but not the analyte. The first step is the ablation of the upper layer of the matrix, producing a hot plume containing several species, such as neutral and ionized matrix molecules, including protonated species, matrix clusters and others. In the second step, the analyte molecules are ionized, usually by protonation, forming the $[M+H]^+$ ions. The increase in molecular mass range when MALDI is used is significant when compared with FAB and LSIMS: 10 000 to 300 000 Da depending on the analyzer used. In all the above mentioned methods, the ionization of the analyte usually gives rise to mono-charged ionic species.

In the case of ESI, a solution of the analyte is introduced through a capillary, at atmospheric pressure, into a small-diameter tip held at potential of approximately 3000V, and is dispersed into a fine aerosol of charged droplets. These droplets pass down potential and pressure gradients towards the analyzer. The evaporation of the solvent from the charged droplets is usually assisted by a nebulizer gas. The size of charged droplets decreases until they become unstable, and form more stable droplets by Coulombic fission. This process of desolvation and fission is repeated until desolvated ions are produced. The typical solvents used in electrospray ionization are prepared by mixing water with volatile organic compounds (methanol or acetonitrile). ESI can produce ions from macromolecules with low internal energy overcoming their propensity to fragment when ionized. ESI is advantageous over other ionization processes (for instance MALDI) since it may produce multiple charged ions, usually $[M+nH]^{n+}$ effectively extending the mass range of the analyzer up to the MDa range. The development of ESI also allowed the effective coupling of mass spectrometry with flow separation techniques such as HPLC (high pressure liquid chromatography).

Following the implementation of electrospray as an ionization technique, other atmospheric pressure ionization methods have been developed, such as APCI and APPI.

APCI is an ionization method analogous to chemical ionization (CI), although it occurs at atmospheric pressure. Similarly to CI, it is not suitable for the analysis of thermally labile compounds. It shares a strong resemblance to electrospray ionization (ESI) and as such is also commonly used in conjunction with HPLC. Unlike ESI, for which the ionization is brought about through the potential difference between a spray capillary (needle) and sampling cone, along with rapid desolvation, in APCI the analyte solution is introduced into a pneumatic nebulizer and desolvated in a heated quartz tube, before being submitted to electrical discharge (corona discharge), creating ions. The corona discharge replaces the electron filament in CI, producing primary ions by electron ionization. The primary ions collide with the vaporized solvent molecules to form secondary reactant gas ions. The later undergo repeated collisions with the analyte molecules, leading to the formation of thermalysed analyte ions, with high ionization efficiency. Very few fragment ions are formed and the mass spectra show predominantly the protonated analyte molecules, $[M+H]^+$, although other adduct ions can be also observed.

Another atmospheric pressure technique is APPI. Similarly to ESI, the liquid solution is vaporized with the help of a nebulizing gas, such as nitrogen, but then it enters in an ionization chamber at atmospheric pressure. There, the mixture of solvent and sample molecules is exposed to photons of ultraviolet light, usually from a krypton lamp (10 eV). This specific energy is enough to ionize the analyte molecules, but not high enough to ionize air components and other surrounding molecules. The photons also excite the solvent molecules and, as the process occurs at atmospheric pressure, these solvent molecules collide with molecules of the analyte. A small fraction of these collisions result in the ionization of the analyte and both the radical cations, $M^{+\cdot}$ and the protonated analyte molecules $[M+H]^+$ can be formed.

To increase the ionization yield of the analyte molecules, dopant-assisted APPI (APPI-d) can be also used. The dopant molecules (usually toluene) are in a large excess relative to the analyte molecules and are directly ionized by the UV photons. The ionized dopant molecules collide with the neutral analyte molecules giving rise to the radical cations, $M^{+\cdot}$ and the protonated analyte molecules $[M+H]^+$.

Mass spectrometry analysis of corroles by ESI-MS

The first report of ESI-MS/MS applied to corroles was the study of 5,10,15-tris(pentafluorophenyl)corrole (T^FPC) **3**, Fig. 2, present as an impurity of 5,10,15,20-tetrakis(pentafluorophenyl)porphyrin (T^FPP).[115]

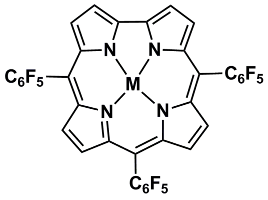

3 M = 3H;
3A M = Cu(III);
3B M = Mn(III);
3C M = Co(III);

Fig. 2 Representative structure of 5,10,15-tris(pentafluorophenyl)corrole (T^FPC) **3** and their respective metal complexes **3A**, **3B** and **3C**.

The product ion spectra of the protonated $[M+H]^+$ (positive ion mode) and deprotonated $[M-H]^-$ (negative ion mode) of T^FPC showed consecutive losses of hydrogen fluoride molecules with formation of direct *o*-phenyl-to-β-linkages, generating fused five-membered fragment ions, similar to those already observed for other porphyrins and porphyrinoids, namely T^FPP, its neutral and cationic pyrrolidine-fused chlorin and isobacteriochlorin derivatives[84] and *meso*-tetra(heptafluoropropyl)porphyrin (T^FHP).[99]

Compared to some of the above mentioned compounds, T^FPC and T^FPP possess simpler structures that enable HF molecule elimination to occur as the only significant loss. The mechanism of this elimination was proposed to be that of a nucleophilic aromatic substitution, common for the pentafluorophenyl group. Computer studies of the relative energies of the ions formed by HF molecule eliminations indicated the occurrence of cooperative interactions between *o*-phenyl-to-β-linkages that occurred in a regioselective unidirectional mode. A good correlation could also be established between the calculated relative energies for each species resulting from HF molecule losses and the relative abundances of its product ions, obtained in the negative ion mode. Thus, the number of HF molecule eliminations observable in the negative ion mode spectra was recognized as a reliable tool for the identification of the number of pentafluorophenyl groups attached to a macrocycle.

Although the HF molecule eliminations were observed both in the positive and in the negative ion modes, the authors found that the fragmentation patterns of deprotonated T^FPC and T^FPP were richer and better defined when using ESI in the negative ion mode.[115]

In the specific case of T^FPC **3**, three consecutive HF molecule eliminations, one from each pentafluorophenyl substituent, lead to species **4A** shown in Fig. 3. Similarly, for T^FPP, four consecutive HF eliminations lead to species **4B** presented in the same Figure. The authors proposed that similar HF eliminations with formation of *o*-phenyl-to-β-linkages were expected to occur for *meso*-pentafluorophenyl substituted porphyrinic and porphyrinoid compounds. They also suggested that ESI-MS/MS could act as a strategic pointer for the bulk synthesis of novel porphyrinoid structures.[115]

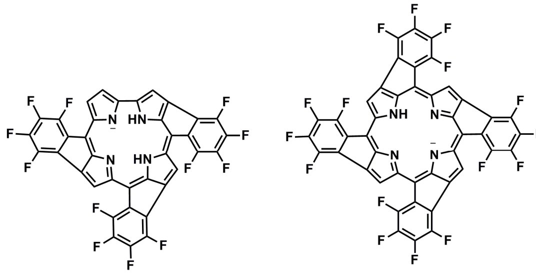
4A **4B**

Fig. 3 Structures of fused fragment ions for T^FPC (**4A**) and T^FPP (**4B**).[115]

ESI is an ionization technique for which solution-phase information is retained into the gas-phase, to the point that very weak non-covalent interactions can be observed. It is thus interesting to compare the reported gas-phase behavior of the $[M+H]^+$ ions of T^FPC and T^FPP and of their $[M-H]^-$ counterparts, with their solution acid-base properties. Like porphyrins, corrole inner-core nitrogen atoms can be both protonated and deprotonated, but neutral corroles have an unusually high N-H acidity when compared to neutral porphyrins.[122] Moreover, solution formation of mono-protonated porphyrins $[M+H]^+$ is not a dominant process, as the doubly-protonated species are formed very rapidly.

The reported advantages of the use of ESI in the negative ion mode[115] may be explained in the case of T^FPC by its easy deprotonation. On the other hand, when the positive ion mode is used, protonated T^FPP is expected to be less stable than protonated T^FPC. Therefore, T^FPC ions are expected to be more stable than their analogous T^FPP species both in the positive and negative ion modes.

The observed similarity of the gas-phase behavior of protonated T^FPC and T^FPP in the positive ion mode and of their deprotonated counterparts in the negative ion mode, is apparently at odds with their solution properties. A probable explanation is that, although solution stability can be directly related to the gas-phase abundance of the $[M+H]^+$ and $[M-H]^-$ ions of T^FPC and T^FPP, their structural similarity may be the cause of their analogous behavior after mass selection and collisional activation.

Danikiewicz, Gryko and collaborators[80] used electrospray and three other ionization techniques, field desorption (FD), atmospheric pressure ionization (APPI) and atmospheric pressure chemical ionization (APCI), to monitor the chemical processes occurring in solutions containing the *meso*-substituted free base corroles **5-10** with electron withdrawing, electron donating and sterically hindered groups (Fig. 4).

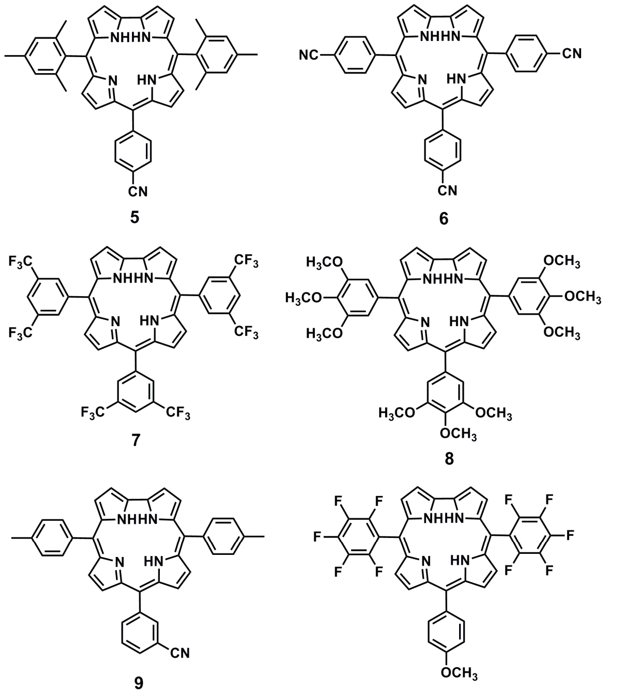
5 **6** **7** **8** **9** **10**

Fig. 4 Structures of different corroles studied by Danikiewicz, Gryko and co-workers.[80]

The authors were especially interested in assessing the purity of the compounds but they also wished to determine the structure of their light- and oxygen-induced oxidation products. The stability of the corroles in a range of solvents (methanol, acetonitrile, ethyl acetate, dichloromethane and hexane) was tested by acquiring their mass spectra immediately after the dilution, 30 minutes and 1 hour later. The solutions were kept at ambient light in contact with air. Contrary to what was expected, it was found that the stability of corroles **5-10** in solvents which contained the highest amount of dissolved oxygen was rather high, whereas for acetonitrile solutions, the ions corresponding to oxidation products were formed with the highest relative abundances. Using the acetonitrile solutions, corrole **10** was found to be the most stable due to the electron withdrawing effect of the pentafluorophenyl groups in the *meso* positions (Fig. 4). Corroles **5** and **8** bearing respectively the sterically hindered substituents bis-mesityl and tris-trimethoxyphenyl were found to lead to the most abundant oxidation products.

The oxidized species of corrole 5,15-bis(mesityl)-10-(4-cyanophenyl)corrole **5** were isolated and characterized by NMR, IR, and identified by their product ion spectra and accurate mass measurements. Based on these data, the authors suggested the following structures for the oxidation products: the isocorrole **11A** and the two biliverdin-like isomers **11B** (major) and **11C** (Fig. 5).

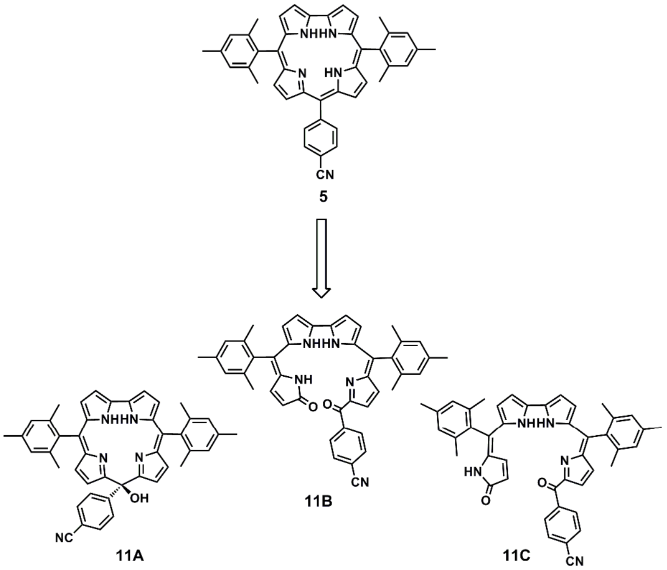

Fig. 5 Structures of oxidized species identified by Danikiewicz, Gryko and co-workers.[80]

Field desorption (FD) was found to be the most suitable ionization method to evaluate the purity degree of corroles whereas oxidation was always induced by electrospray ionization even when the corrole samples were pure.

Danikiewicz, Gryko, Lewtak and Swider[104] selected porphyrins **12**-**17**, corroles **5**, **8**, **18**-**22** and the cyanocobalamins **23** and **24** (see structures in Figs. 4 and 6) to evaluate the ionization efficiency of three atmospheric pressure ionization techniques, ESI, APCI and APPI using toluene as a dopant (APPI-d) in order to acquire useful information for the design of future MS or liquid chromatography-MS experiments. The relative sensitivity of the above mentioned ionization techniques was assessed both in the negative and positive ion modes by evaluating the relation between the instrumental response (represented by peak area) and the analyte concentration.

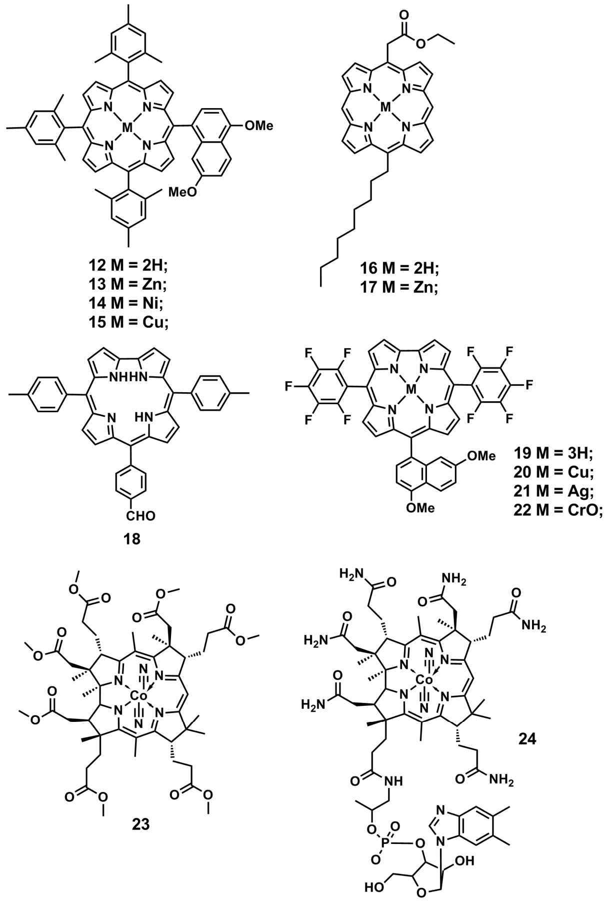

Fig. 6 Structures of different tetrapyrrolic macrocycles studied by Danikiewicz, Gryko and co-workers.[104]

In the positive ion mode, the highest sensitivity was achieved for the free-base porphyrins (**12** and **16**) and corroles (**5**, **8**, **18** and **19**) when using ESI, as well as for the cyanocobalamin **23** and its derivative **24**. For the same free-base compounds APCI and APPI-d gave similar results although a slightly better sensitivity was achieved for the free-base porphyrins when using APPI-d. A different situation was observed for cyanocobalamin **23** and its derivative **24** where higher sensitivity was observed for APCI than for APPI-d. For metalloporphyrins **13**-**15** and **17**, APCI and APPI-d provided better sensitivity than ESI. For metallocorroles **20**-**22** no common pattern concerning the sensitivity of the API methods was found.[104]

When compared with the positive ion mode, a higher sensitivity was observed for all corroles, in the negative ion mode, for all the ionization techniques. In the case of the free base corroles, **18** and **19**, this feature is explained by their higher acidity[122] when compared, for instance, with the free base porphyrins **12** and **16**. The higher ability of metallocorroles to form anions, which has led to their trial as anion sensors[25,123] may explain the higher sensitivity observed.

In the negative mode ESI proved to be much more sensitive than APCI and APPI-d techniques. For the metalloporphyrins, with exception of zinc complexes **13** and **17**, APPI-d was the most sensitive ionization method, in the negative ion mode, although for all the studied porphyrins, sensitivity in this mode was lower than in the positive ion mode.

For both ion modes, ESI was shown to be the best ionization technique for cyanocobalamins, free-base corroles and porphyrins, whereas for metallocorroles and metalloporphyrins, APPI-d proved to be the best one.

When compared with porphyrins, corroles have a higher tendency to generate anions by electron capture in mass spectrometry sources. On the other hand, electron capture is a practical technique for the generation of peptide radicals. The special redox properties of corroles, namely their high tendency to generate anions by electron capture in electrospray sources, were used by Denekamp and Rabkin[89] for the gas-phase generation of anion radicals in amino acid esters corroles **25**-**36** (Fig. 7), in order to induce the initiation of homolytic cleavages at the α-carbon of the amino acid ester chain.

In a first approach, complexes of 5,10,15-tris(phenyl)corrole (TPC) with Fe, Mn, Co, Ni, Cr, Pd, Ag and Cu were mass analysed, by MALDI and ESI, and cation and anion radical formation was observed for all of them, with both techniques.[89] A charge derivatization reagent must be stable upon collisional activation, thus MS/MS experiments were conducted for all of the above mentioned metallocorroles. The most stable ions were, as expected, the negatively charged copper and nickel complexes. Due to synthetic limitations, only the copper complex was used. Moreover the later is a d^8 complex that upon electron capture becomes an open shell d^9 species required to initiate homolytic processes. Derivatization was applied on a variety of amino acid esters, affording complexes that were easily ionized into stable radical anions. The derivatized amino acids were collisionally induced to dissociate, forming a series of fragments, some of which indicating cleavages at the α-carbon with the involvement of the alkyl side chain as desired.

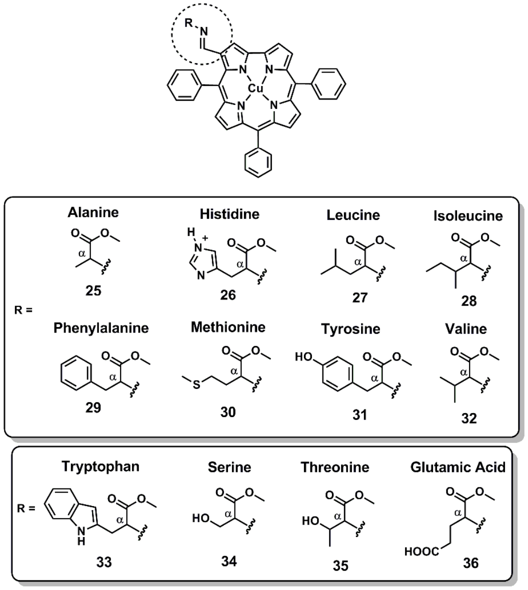

Fig. 7 Structures of substituted Cu(III)-corrolates with amino acid esters studied by Denekamp and co-workers.[89]

The various anion radicals can be formed from two main groups of compounds: the first group, which includes the esters of alanine, histidine, leucine, and isoleucine, phenylalanine, methionine, tyrosine and valine, can lose a radical moiety, giving rise to a closed-shell product ion; the second group, that includes the esters of tryptophan, serine, threonine and glutamic acid can eliminate a closed-shell neutral species, giving radical product ions. The exception was lysine that did not afford informative side chain fragmentations.

Almost all the product ion spectra of the $M^{-\cdot}$ ions of the derivatized amino acids showed fragments corresponding to the cleavage at the α-carbon either with, or without, the loss of the alkoxy ester moiety. The cleavages of N-Cα bonds occurred after carbonyl hydrogen abstraction and the active species for radical induced fragmentation were proposed to be located at the carbonyl that leaves off the R-Cα alkyl chain or at the corrole backbone.

Gas-phase coordination chemistry of metalloporphyrinoids

The formation metalloporphyrinoids in the source was studied by FAB mass spectrometry for *meso*-tetra(aryl)porphyrins **37**-**40** and for the *meso*-tetra(phenyl)chlorin **41** (Fig. 8).[83,84] In this study the authors used divalent salts of Mg, Fe, Co, Ni, Cu, Zn, Cd and Pb and a trivalent salt of Fe(III). The formation of metalloporphyrin and metallochlorin ions was observed for all the compounds tested, except for the Mg(II), Fe(II), Fe(III) and Ni(II) salts. The analysis of the relative abundances of the PH_3^+ and $MetP^{+\cdot}$ ions formed from mixtures of the free bases, PH_2, and of the corresponding metallated compounds, MetP, indicated that metalloporphyrin formation under FAB was predominantly a solution process, as the PH_3^+ ions were formed with higher relative abundances than the corresponding $MetP^{+\cdot}$ ions, indicating that desorption of the former was easier.

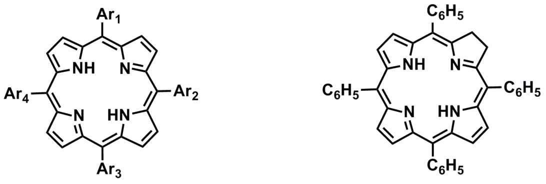

41

37 $Ar_1 = Ar_2 = Ar_3 = Ar_4 = H$;
38 $Ar_1 = NO_2$; $Ar_2 = Ar_3 = Ar_4 = H$;
39 $Ar_1 = COOCH_3$; $Ar_2 = Ar_3 = Ar_4 = H$;
40 $Ar_1 = Ar_2 = Ar_3 = Ar_4 = OCH_3$;

Fig. 8 Structures of *meso*-tetra(aryl)porphyrins **37-40** and of *meso*-tetra(phenyl)chlorin **41**.[83,84]

UV-visible absorption spectroscopy was also used to study their formation in solution and similar results to those obtained by FAB were attained, showing that the interactions with the matrix did not play a predominant role in metalloporphyrin formation under FAB. Differences in the metal counter ion were also found to influence the overall metalloporphyrin formation. A comparison with solution chemistry behaviour through the use of static solution coordination parameters did not lead to a complete explanation of the observed results, showing that kinetic parameters had to be considered.

In the case of metallocorroles their formation by electrospraying solutions of T^FPC **3** (Fig. 2) and divalent and trivalent metal cations, in their acetate salt form, and also by desorption of these solutions from liquid matrices was investigated.[117] The isotopic patterns of the metallocorrole ions formed by these processes were compared to those of the corresponding metallocorrole ions formed from previously synthesized metallocorroles. The authors selected divalent metal acetates such as Mn(II), Co(II), Cu(II), Zn(II) and also the trivalent Mn(III) acetate, in order to investigate the influence of the oxidation state of the metal ion on metallocorrole formation in the source, and, concurrently, if oxidation of the divalent ions could occur during the ionization process.

This allowed not only a comparison of solution and gas-phase coordination chemistry, but also the acquisition of information on the ionization processes either in the case of liquid secondary ion mass spectrometry (LSIMS) or electrospray mass spectrometry (ESI-MS).

When using LSIMS the molecular ion peaks corresponding to the metallocorrole ions $MC^{+\cdot}$, of the tested metal salts were obtained. From the analysis of the experimental and calculated isotopic patterns it was established that $M(III)C^{+\cdot}$ were formed for all salts except when using Zn(II) acetate. The isotopic patterns, both experimental and calculated for the synthesized metallocorrole **3A**, **3B** and **3C** ions (Fig. 2) were also obtained and were identical with those of the corresponding ions formed in the source.

When using ESI spectra in the positive ion mode the formation of the $M(III)C^{+\bullet}$ ions, when Mn(II), Co(II) and Cu(II) acetates were used, was predominant. However, in the presence of Zn(II) acetate, the ion corresponding to $M(II)C^{+}$ was formed with low relative abundance, whereas the $M(II)CH^{+\bullet}$ ion was much more abundant. When using Mn(III) acetate the formation of metallocorrole ions was not detected. The acquired data pointed to oxidation of the metal centre, in the source, during the formation of metallocorrole positive ions, in the case of divalent metal cations.

When the studies were performed by ESI in the negative ion mode, the $M(II)C^{-}$ ions were observed for T^FPC **3** with Mn(II), Co(II), Cu(II) and Zn(II) acetates. In the ESI spectra of the metallocorroles **3A**, **3B** and **3C** synthesized by classical procedures, ions with the same *m/z* values as the ions formed in the source were observed (Fig. 2).

Based on the obtained data a mechanism for the formation of the metallocorrole ions $M(III)C^{+\bullet}$ either by LSIMS or electrospray in the positive ion mode was proposed. It involved a stepwise proton-to metal substitution (**eq. a**, **b**, **c**, **d**), assisted by the acetate ions, followed by oxidation (**eq. e**, **f**, **g**). In the case of ESI in the negative ion mode only the $M(II)C^{-}$ ions were detected, as further oxidation was prevented by the negative needle potential.[117]

$$H_3C + M^{2+} \longrightarrow M(II)CH_3^{2+} \qquad (a)$$

$$M(II)CH_3^{2+} \longrightarrow M(II)CH^{2+} + H^{+} \qquad (b)$$

$$M(II)CH^{2+} \longrightarrow M(II)CH^{+} + H^{+} \qquad (c)$$

$$M(II)CH^{+} \longrightarrow M(II)C^{-} + H^{+} \qquad (d)$$

$$M(II)CH^{+} \longrightarrow M(II)C^{+\cdot} + e^{-} \qquad (e)$$

$$M(II)C^{-} \longrightarrow M(III)C + e^{-} \qquad (f)$$

$$M(III)C \longrightarrow M(III)C^{+\cdot} + e^{-} \qquad (g)$$

Where H_3C = Corrole **3** and M = Mn(II); Co(II); Cu(II) or Zn(II);

For the metallocorroles **3A**, **3B** and **3C** synthesized under classical conditions, the formation of the $M(III)C^{+\bullet}$ and $M(III)CH^{+}$ ions, in the positive ion mode, must occur by electron removal and protonation of the neutral corroles, respectively. In the negative ion mode, electron attachment with formation of the $M(III)C^{-\bullet}$ radical anions was observed.

The complex ionization mechanism proposed can be further justified if the electrolytic nature of electrospray processes, put forward two decades ago[124-126] and generally accepted, despite some controversy,[127] is taken into account. A study on the electrochemistry of *meso*-substituted free-base corroles, including T^FPC,[128] has shown that the prevailing mechanisms for the oxidation and reduction of free base H_3C corroles are the formation of species such as H_2C^{-}, $[H_2C^{\bullet}]^{2-}$, $H_2C^{\bullet}$, H_2C^{+}, $[H_2C]^{3-}$ $[H_3C^{\bullet}]^{+}$, $[H_3C^{\bullet}]^{-}$, H_4C^{+}, $H_4C^{\bullet}$ and $[H_4C^{\bullet}]^{2+}$ depending on the solvents used, portraying a multistep process involving protonation, deprotonation and one electron transfer.

The product ion spectra of the metallocorrolle ions formed in the source and from previously synthesized metallocorroles were identical, for each metal centre. The main fragmentation pathway for the metallocorrole ions was via elimination of one to three HF molecules.

Corrole isomer differentiation by ESI-MS

Isomer differentiation using ESI-MS/MS can be accomplished if the product ions of the isomers, positional, diastereoisomers and others, have different *m/z* values or if they have the same *m/z* values, but different relative abundances.[93,121] In general, isomer differentiation by ESI-MS/MS is not straightforward and it is often based on the formation of adducts, complexes or derivatized species, either in the source[129,130] or before the introduction into the mass spectrometer and in many instances, multiple stage mass analysis MS^n (n>2) is required.[131-133]

Two β-(aminomethyl)gallium(III) T^FPC isomeric derivatives **42A** and **42B** (Fig. 9) were successfully differentiated, using ESI in the positive and in the negative ion modes.[116]

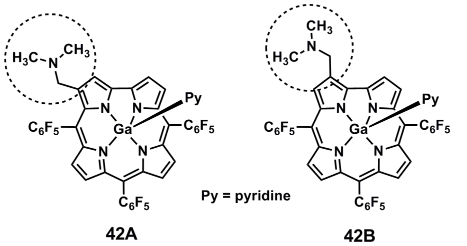

42A **42B**

Fig. 9 Structures of studied β-(aminomethyl)gallium(III) derivatives.[116]

This was accomplished, in the positive ion mode, through two types of diagnostic ions, the first formed by loss of a neutral dimethylamine molecule $[(M\text{-py}) - NH(CH_3)_2]^{+}$, corresponding to the base peak in the mass spectra, and the second, the $[(M\text{-py}) - NH(CH_3)_2 + H_2O]^{+}$ ion resulting from an unusual addition of one water molecule to the former. Accurate mass measurements, multistage mass spectrometry ESI-MS^n (n>2) and energy-resolved MS, were also used to investigate the formation and structure of the above mentioned diagnostic ions. In the negative ion mode, isomer discrimination was achieved through the fragmentation of the methoxide adduct ions $[(M\text{-py}) + CH_3O]^{-}$.

In the positive ion mode, the product ion spectra of the fragment ions formed by dimethylamine molecule elimination, $[(M\text{-py}) + H - NH(CH_3)_2]^{+}$, showed losses of HF molecules for the two isomers, but the relative abundances of the fragment ions formed by the loss of one HF molecule, $[(M\text{-py}) + H - NH(CH_3)_2 - HF]^{+}$, are quite different, indicating the formation of two isomeric ions with different stabilities.

Two different structures for the ions formed by HF loss were proposed: a six-membered ring **44** (Scheme 1, above) and a five-membered ring **46** (Scheme 1, below) similar to previously described structures.[84,99,115]

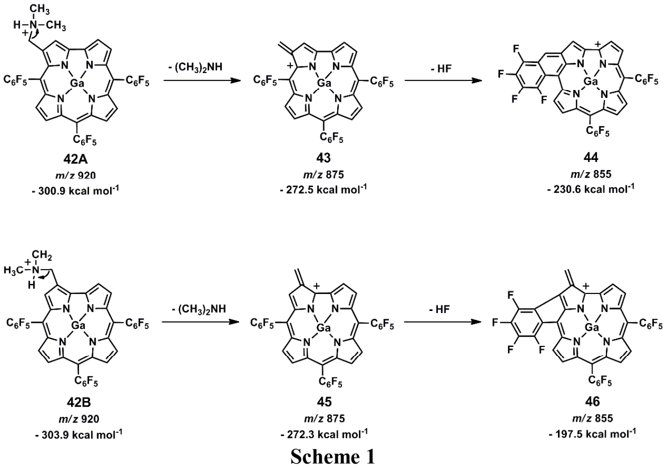

Scheme 1

The observed difference in stabilities was found to be consistent with data obtained from semi-empirical calculations. The calculated formation enthalpy values for the ions $[(M\text{-py}) + H]^{+}$ and $[(M\text{-py}) + H - NH(CH_3)_2]^{+}$ were similar for both isomers, but the calculated formation enthalpies for the $[(M\text{-py}) + H - NH(CH_3)_2 - HF]^{+}$ ions, shown in Scheme 1, were different: for the $[(M\text{-py}) + H - NH(CH_3)_2 - HF]^{+\bullet}$ structure, shown above; the calculated formation enthalpy is -230.6 kcal mol^{-1} for **44**, whereas for the isomeric structure below, **46**, the formation enthalpy is -197.5 kcal mol^{-1}. Isomer differentiation could also be achieved through the MS^3 spectra corresponding to the sequence $[(M\text{-py}) + H]^+ \rightarrow [M\text{-py} + H - NH(CH_3)_2]^+ \rightarrow$ product ions.

In the negative ion mode, differentiation can be achieved through the product ion spectra of the $[(M\text{-py}) + CH_3O]^-$ ions, (represented as M'^-) formed from methanol used as the eluent. The differences between the two spectra are self-evident: the base peak corresponds to the $[M' - (CH_3)_2N - HF]^{-\bullet}$ ions, for one of the isomers and to the $[M' - (CH_3)_2N]^{-\bullet}$ ions, for the other (Fig. 10).

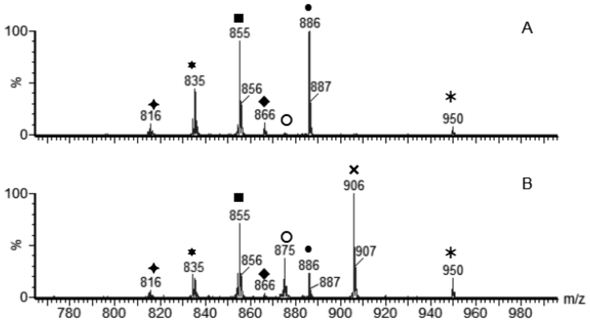

Fig. 10 Product ion spectra of the ions $[(M\text{-py}) + CH_3O]^-$ (A – isomer **42A** and B – isomer **42B**). * - precursor ion; X – $[M' - (CH_3)_2N]^{\bullet-}$; • - $[M' - (CH_3)_2N^\bullet - HF]^{\bullet-}$; ○ – $[M' - (CH_3)_2N^\bullet - CH_3O^\bullet]^-$; ♦ - $[M' - (CH_3)_2N^\bullet - 2HF]^{-\bullet}$; ■ – $[M' - (CH_3)_2N^\bullet - HF - CH_3O^\bullet]^-$; ∗ - $[M' - (CH_3)_2N^\bullet - 2HF - CH_3O^\bullet]^-$ and ✦ - $[M' - (CH_3)_2N^\bullet - 3HF - CH_3O^\bullet]^-$. (Reproduced/Adapted from reference 116).

Besides the HF losses, the main fragment ions are formed by losses of dimethylamino radicals $(CH_3)_2N^\bullet$, by themselves, or as joint losses with HF molecules and methoxide radicals, $CH_3O^\bullet$.
The formation of the $[M' - (CH_3)_2N - HF]^{-\bullet}$ ions can be explained by a mechanism involving the formation of a six-membered fused ring for isomer A (corrole **42A**), similar to the one proposed for their positive ion counterpart. As this process is not available in isomer B (corrole **42B**) loss of a $(CH_3)_2N^\bullet$ radical is the preferred process. ESI-MS/MS, in combination with NMR analysis, was also used to differentiate the two free-base galactopyranose-tris(pentafluorophenyl)corrole positional isomers **47A** and **47B** (Fig. 11).[54]

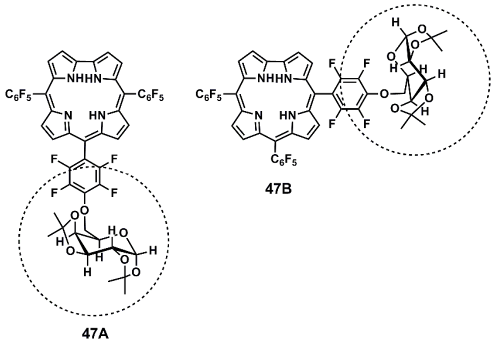

Fig. 11 Structure of galactopyranose-tris(pentaflurophenyl)corrole positional isomers.[54]

The product ion spectra of the $[M+H]^+$ ions of the isomeric pair **47A**, **47B**, formed by electrospray ionization, showed fragment ions with the same *m/z* values. However the two most abundant product ions, $[M + H - (Gal\text{-}H)]^+$ and $[M + H - (Gal\text{-}H) - HF]^+$, were formed with different relative abundances for each isomer. The first ion was formed by cleavage of the C–O bond and migration of one hydrogen to the oxygen of the ether bond by a mechanism already described for glyco-tetrakis(pentafluorophenyl)porphyrin derivatives.[134,135] The second ion resulted from a joint loss of the former fragment and a HF molecule. Loss of HF occurs with formation of direct *o*-phenyl-to-β-linkages as discussed above.

Recently, the techniques of ion mobility spectrometry (IMS) and ion mobility spectrometry coupled to mass spectrometry (IM–MS) are being used with success in isomer differentiation.[118-120] Ion mobility mass spectrometry, which is becoming increasingly popular, provides high sensitivity, specificity, and analysis times on millisecond time range. Besides the usual mass and charge parameters, the separation in IM–MS is also based on analyte shape (measured by its collision cross section) which affects its interactions with gases throughout a drift tube.[136-140] More recently the technique of TWIM-MS was developed. Unlike conventionally IMS, in which an electric field is, applied continuously, TWIM uses continuous transient voltage pulses.[141]

Eberlin and collaborators[119] used this technique in the positive ion mode to study mixtures containing the isomeric *meta*/*para* and *adj*/*opp* ruthenated *meso*-(pyridyl)porphyrins **48**-**59** (Fig. 12). The more compact *meta* positional isomers were found to display shorter drift times than the *para* isomers, and the separation was substantially increased for the multiply charged species. The isomers displayed very close drift times both in CO_2 and N_2 and TWIM-MS was unable to differentiate these porphyrin isomers.

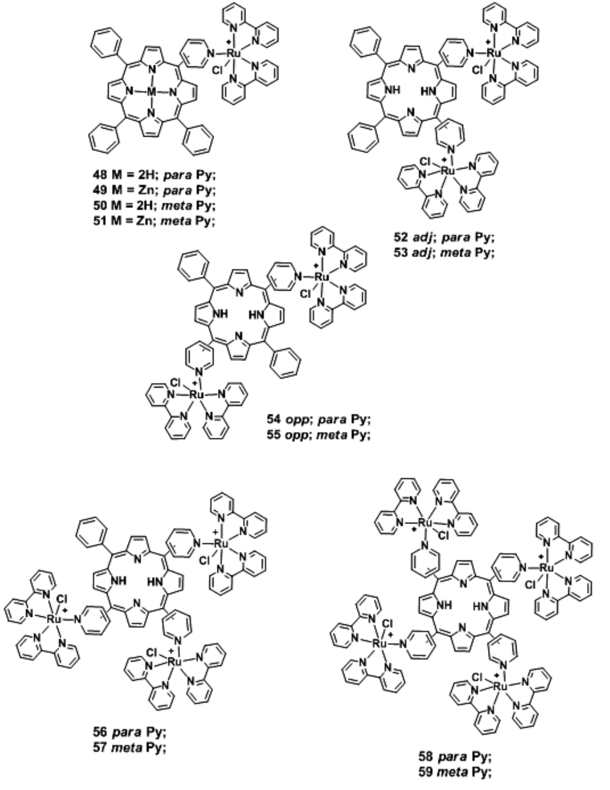

Fig. 12 Structures of ruthenium(II)-porphyrinato complexes **48**-**59**.[119]

Eberlin and co-workers[120] also used the ESI coupled to TWIM analysis to investigate the protonation and deprotonation sites of *meso*-tetra(pyridyl) and *meso*-tetrakis(carboxyphenyl)porphyrins **60**-**62** (Fig. 13), both in the positive and negative ion modes. In the positive ion mode, for the *meso*-tetra(pyridyl)porphyrins **60** and **61**, two different protonation sites were identified: the first, in one of the inner nitrogens and the second, in one of the *N*-pyridyl substituents.

A similar behaviour was observed, in the negative ion mode, for *meso*-tetrakis(carboxyphenyl)porphyrin **62**, where two "*de-protomers*" were identified, the first resulting from deprotonation of an inner nitrogen and the second from a carboxyl substituent.

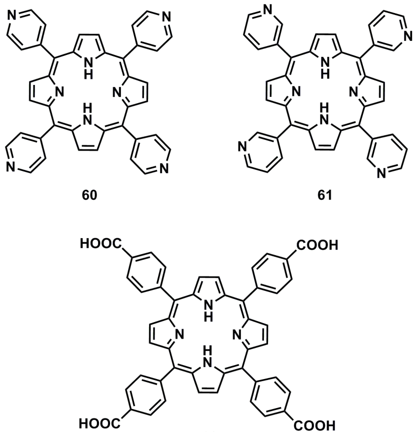

60 **61**

62

Fig. 13 Structures of *meso*-tetra(pyridyl)porphyrins **60**-**61** and *meso*-tetrakis(carboxyphenyl)porphyrin **62**, respectively.[120]

Corrole **3** and four of its isomers **63**-**66** (Fig. 14), with subtle structural changes were also studied by Eberlin and collaborators,[118] using travelling wave ion mobility mass spectrometry (TWIM-MS) and collision induced dissociation (CID) of electrosprayed ions.

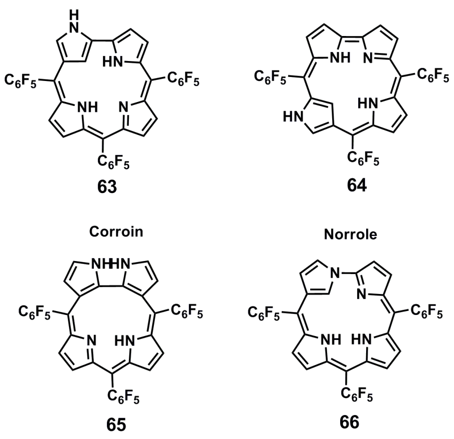

Fig. 14 Structures of corrole **3** isomers studied by Eberlin and co-workers.[118]

In this work, the relative gas-phase mobilities of the five protonated isomers were evaluated by TWIM-MS using two drift gases, N_2 and CO_2. When N_2 was used, corroin **65** was the isomer with the higher mobility followed by norrole **66**, *N*(2)-confused corrole **64** and *N*(4)-confused corrole **63**, with similar drift times and finally by corrole **3** (Fig. 16). When CO_2, with higher polarizability and mass, was used as drift gas, corroin **65** presented a much higher mobility and the mobility of corrole **3** was higher than that of *N*(4)-confused corrole **63** (Fig. 15).

As the charge is the same for all the protonated isomers and the calculation of the collision cross sections using density functional theory calculation (DFT) led to a tight range of values, ion-induced dipole interactions were responsible for the different mobilities observed, especially when CO_2 was used as drift gas. DFT calculations showed that corroin **65** possesses the most compact tridimensional structure, as expected from its shorter drift times (Fig. 15).

Sequential losses of HF molecules were observed in the product ion spectra of the protonated molecules of these isomers, as observed before by Furuta and collaborators.[113] *N*(4)-confused corrole **63** showed a unique and diagnostic extensive loss of a NH_3 molecule, which allowed its rapid differentiation from the other isomers.

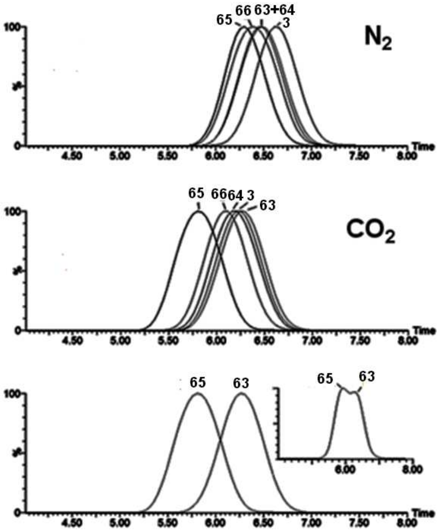

Fig. 15 TWIM drift time graphical plots obtained for the protonated isomers analysed: *N*(4)-confused corrole **63**, *N*(2)-confused corrole **64**, corroin **65**, norrole **66** and corrole **3**, respectively. (Reproduced/Adapted from reference 118).

Conclusions

The importance of electrospray ionization mass spectrometry in the analysis of corrole derivatives is well illustrated by the range of examples discussed in this review. Fragmentation and degradation mechanisms, identification of new compounds and macrocycle structure characterization were some of the areas where ESI-MS played an important role. The increase in the number of publications in this field is also a pointer of the importance of this technique. On the other hand, the still limited number of publications on specific aspects of corrole gas-phase chemistry shows that novel applications of this technique can still be developed.

It is predictable that ESI, specially when used with TWIM analyzers, will be the technique of choice for the analysis, not only of corrole isomers, but of corrole based complex structures, such as corrole-porphyrin dimers, corrole adducts with biomolecules and other supramolecular structures, either covalently linked or resulting from solution self-assembly.

Previous studies of the adducts of G-quadruplex DNA and cationic corrole isomers by circular dichroism (CD) and temperature melting assays showed that these compounds are G-quadruplex stabilizers and thus potential candidates for new anticancer drugs. It is probable that ESI -TWIM-MS will be used in the future, for the design and development of corrole based anticancer drugs, including the implementation of screening techniques.

Besides ESI, other recently developed ionization techniques such as easy ambient sonic spray ionization (EASI-MS) which can be used directly from layer chromatography (TLC) plates are extremely promising for the identification of products from corrole syntheses.

Acknowledgements

We would like to thank Fundação para a Ciência e a Tecnologia (FCT, Portugal), the European Union, QREN, FEDER, COMPETE, for funding the Organic Chemistry Research Unit (QOPNA) (project PEst-C/QUI/UI0062/2013; FCOMP-01-0124-FEDER-037296). J. F. B. Barata and C. I. V. Ramos also thank Fundação para a Ciência e Tecnologia (FCT) for the grants SFRH/BPD/63237/2009 and SFRH/BPD/85902/2012, respectively. B. A. Iglesias also thanks Conselho Nacional de Desenvolvimento Científico e Tecnológico (CNPq – Brazil) for the grant 200802/2012-7.

Notes and references

Department of Chemistry and QOPNA, University of Aveiro, 3810-193 Aveiro, Portugal. Tel:+351234370717; E-mails: bernardopgq@gmail.com and jcavaleiro@ua.pt

1 H. Fisher and K. Zeile, *Liebigs Ann. Chem.*, 1929, **468**, 98-116.

2 R. B. Woodward, W. A. Ayer, J. M. Beaton, F. Bickelhaupt, R. Bonnett, P. Buchschacher, G. L. Closs, H. Dutler, J. Hannah, F. P. Hauck, S. Itô, A. Langemann, E. Le Goff, W. Leimgruber, W. Lwowski, J. Sauer, Z. Valenta and H. Voltz, *J. Am. Chem. Soc.*, 1960, **82**, 3800-3802.

3 A. W. Johnson and R. Price, *J. Chem. Soc.*, 1960, 1649-1653.

4 A. W. Johnson and I. T. Kay, *J. Chem. Soc.*, 1965, 1620-1629.

5 R. K. Pandey and G. Zheng in *Porphyrins as Photosensitizers in Photodynamic Therapy, The Porphyrin Handbook*, Academic Press, (Ed.), San Diego, 2000, **6**, 157-225.

6 T. Aida and S. Inoue in *Metalloporphyrins as Catalysts for Precision Macromolecular Synthesis, The Porphyrin Handbook*, Academic Press, (Ed.), San Diego, 2000, **6**, 133-155.

7 J. -H. Chou, M. E. Kosal, H. S. Nalwa, N. A. Rakow and K. S. Suslick in *Applications of Porphyrins and Metalloporphyrins to Materials Chemistry, The Porphyrin Handbook*, Academic Press, (Ed.), San Diego, 2000, **6**, 43-131.

8 (a) S. Nardis, D. Monti and R. Paolesse, *Mini Rev. Org. Chem.*, 2005, **2**, 355-374; (b) R. Paolesse, *Synlett*, 2008, **15**, 2215-2230.

9 Z. Gross, N. Galili and I. Saltsman, *Angew. Chem. Int. Ed.*, 1999, **38**, 1427-1429.

10 R. Paolesse, L. Jaquinod, D. J. Nurco, S. Mini, F. Sagone, T. Boschi and K. M. Smith, *Chem. Commun.*, 1999, 1307-1308.

11 D. T. Gryko and B. Koszarna, *Org. Biomol. Chem.*, 2003, **1**, 350-357.

12 B. Koszarna and D. T. Gryko, *J. Org. Chem.*, 2006, **71**, 3707-3717.

13 D. T. Gryko, *Eur. J. Org. Chem.*, 2002, 1735–1743.

14 J. F. B. Barata, C. I. M. Santos, M. G. P. M. S. Neves, M. A. F. Faustino and J. A. S. Cavaleiro in *Synthesis and Modification of Porphyrinoids, Topics in Heterocyclic Chemistry*, Springer-Verlag, Berlin, 2014, **33**, 79-141.

15 I. Aviv-Harel and Z. Gross, *Chem. Eur. J.*, 2009, **15**, 8382-8394.

16 L. Flamigni and D. T. Gryko, *Chem. Soc. Rev.*, 2009, **38**, 1635–1646.

17 I. Aviv and Z. Gross, *Chem Commun.*, 2007, 1987-1999.

18 K. Kurzatkowska, E. Dolusic, W. Dehaen, K. Sieroń-Stołtny, A. Sieroń and H. Radecka, *Anal. Chem.*, 2009, **81**, 7397–7405.

19 J. -M. Barbe, G. Canard, S. Brandès and R. Guilard, *Angew. Chem.Int. Ed.*, 2005, **44**, 3103–3106.

20 M. Tasior, D. T. Gryko, J. Shen, K. M. Kadish, T. Becherer, H. Langhals, B. Ventura and L. Flamigni, *J. Phys. Chem., C,* 2008, **112**, 19699-19709.

21 Z. Gross and H. B. Gray, *Adv. Synth. Catal.*, 2004, **346**, 165–170.

22 Z. Okun, L. Kupershmidt, T. Amit, S. Mandel, O. Bar-Am, M. B. H. Youdim and Z. Gross, *ACS Chem. Biol.*, 2009, **4**, 910–914.

23 J. F. B. Barata, A. L. Daniel-da-Silva, M. G. P. M. S. Neves, J. A. S. Cavaleiro and T. Trindade, *RSC Advances*, 2013, **3**, 274-280.

24 C. I. M. Santos, E. Oliveira, J. C. Menezes, J. F. B. Barata, M. A. F. Faustino, V. Ferreira, J. A. S. Cavaleiro, M. G. P. M. S. Neves and C. Lodeiro, *Tetrahedron*, 2013, in press, DOI: 10.1016/j.tet.2013.07.022.

25 C.I.M. Santos, E. Oliveira, J. F. B. Barata, M. A. F. Faustino, J. A. S. Cavaleiro, M.G.P.M.S. Neves and C. Lodeiro, *J. Mater. Chem.*, 2012, **22**, 13811-13819.

26 C. I. M. Santos, E. Oliveira, J. Fernandez-Lodeiro, J. F. B. Barata, S. Santos, M. A. F. Faustino, J. A. S. Cavaleiro, M.G.P.M.S. Neves and C. Lodeiro, *Inorg. Chem.*, 2013, **52**, 8564-8572.

27 (a) N. S. Hush, J. M. Dyke, M. L. Williams and I. S. Woolsey, *J. Chem. Soc. Dalton Trans.*, 1974, 395-399; (b) A. Ghosh and K. Jynge, *Chem. Eur. J.*, 1997, **3**, 823-833.

28 Y. B. Ivanova, V. A. Savva, N. Z. Mamardashvili, A. S. Starukhin, T. H. Ngo, W. Dehaen, W. Maes and M. M. Kruk, *J. Phys. Chem. A*, 2012, **116**, 10683-10694.

29 J. L. Sessler and S. J. Weghorn in *Expanded, Contracted & Isomeric Porphyrins,* Tetrahedron Organic Chemistry Series, Pergamon, (Ed.), New York, 1997, **18**, 11-120.

30 H. Palmer in *Molecular electronic structures of transition metal complexes I*, Structure and Bonding Series, Springer, (Ed.), Berlin, 2012, **142**, 49-90.

31 J. A. S. Cavaleiro, A. C. Tomé and M.G.P.M.S. Neves in *Handbook of Porphyrin Science*, World Scientific, (Ed.), Singapore, 2010, **2**, 193–294.

32 P. Rothemund, *J. Am. Chem. Soc.*, 1935, **57**, 2010–2011.

33 J. P. Collman and R. A. Decréau, *Tetrahedron Lett.,* 2003, **44**, 1207-1210.

34 P. Kumari and S. M. S. Chauhan, *J. Heterocycl. Chem.*, 2008, **45**, 779-783.

35 H. Y. Zhan, H. Y. Liu, H. J. Chen and H. F. Jiang, *Tetrahedron Lett.*, 2009, **50**, 2196-2199.

36 A. Mahammed, M. Botoshansky and Z. Gross, *Dalton. Trans.*, 2012, **41**, 10938-10940.

37 J. Vestfrid, M. Botoshansky, J. H. Palmer, A. C. Durrell, H. B. Gray and Z. Gross, *J. Am. Chem. Soc.*, 2011, **133**, 12899-12901.

38 R.-B. Du, C. Liu, D.-M. Shen, Q.-Y. Chen, *Synlett,* 2009, **16**, 2701-2705.

39 S. Nardis, F. Mandoj, R. Paolesse, F. R. Fronczek, K. M. Smith, L. Prodi, M. Montalti and G. Battistini, *Eur. J. Inorg. Chem.*, 2007, 2345-2352.

40 J. H. Palmer, M. W. Day, A. D. Wilson, L. M. Henling, Z. Gross and H. B. Gray, *J. Am. Chem. Soc.*, 2008, **130**, 7786-7787.

41 G. Golubkov, J. Bendix, H. B. Gray, A. Mahammed, I. Goldberg, A. J. DiBilio and Z. Gross, *Angew. Chem. Int. Ed.*, 2001, **40**, 2132-2134.

42 S. Nardis, G. Pomarico, F. Mandoj, F. R. Fronczek, K. M. Smith, and R. Paolesse, *J. Porphyrins Phthalocyanines,* 2010, **14**, 752-757.

43 A. Mahammed, I. Goldberg and Z. Gross, *Org. Lett.*, 2001, **3**, 3443-3446.

44 A. Mahammed and Z. Gross, *J. Porphyrins Phthalocyanines*, 2010, **14**, 911-923.

45 Z. Gross and A. Mahammed, *J. Porphyrins Phthalocyanines*, 2002, **6**, 553-555.

46 I. Saltsman, A. Mahammed, I. Goldberg, E. Tkachenko, M. Botoshansky and Z. Gross, *J. Am. Chem. Soc.,* 2002, **124**, 7411-7420.

47 M. Stefanelli, M. Mastroianni, S. Nardis, S. Licoccia, F. R. Fronczek, K. M. Smith, W. Zhu, Z. Ou, K. M. Kadish and Paolesse, *Inorg. Chem.,* 2007, **46**, 10791-10799.

48 S. Nardis, M. Stefanelli, P. Mohite, G. Pomarico, L. Tortora, M. Manowong, P. Chen, K. M. Kadish, F. R. Fronczek, G. T. McCandless, K. M. Smith and R. Paolesse, *Inorg. Chem.*, 2012, **51**, 3910-3920.

49 M. Mastroianni, W. Zhu, M. Stefanelli, S. Nardis, F. R. Fronczek, K. M. Smith, Z. Ou, K. M. Kadish and Paolesse, *Inorg. Chem.,* 2008, **47**, 11680-11687.

50 M. Stefanelli, F. Mandoj, M. Mastroianni, S. Nardis, P. Mohite, F. R. Fronczek, K. M. Smith, K. M. Kadish, X. Xiao, Z. Ou, P. Chen and R. Paolesse, *Inorg. Chem.,* 2011, **50**, 8281-8292.

51 J.-M. Barbe, G. Canard, S. Brandès and R. Guilard, *Eur. J. Org. Chem.,* 2005, 4601-4611.

52 J. P. Collman and R. A, Decréau, *Org. Lett.,* 2005, **7**, 975-978.

53 T. Hori and A. Osuka, *Eur. J. Org. Chem*., 2010, 2379-2386.

54 T. A. F. Cardote, J. F. B. Barata, M. A. F. Faustino, A. Preuß, M. G. P. M. S. Neves, J. A. S. Cavaleiro, C. I. V. Ramos, M. G. O. Santana-Marques and B. Röder, *Tetrahedron Lett*., 2012, **53**, 6388-6392.

55 J. F. B. Barata, A. M. G. Silva, M. A. F. Faustino, M. G. P. M. S. Neves, A. C. Tomé, A. M. S. Silva and J. A. S. Cavaleiro, *Synlett*, 2004, **7**, 1291-1293.

56 L. S. H. P. Vale, J. F. B. Barata, C. I. M. Santos, M. G. P. M. S. Neves, M. A. F. Faustino, A. C. Tomé, A. M. S. Silva, F. A. A. Paz and J. A. S. Cavaleiro, *J. Porphyrins Phthalocyanines,* 2009, **13**, 358-368.

57 C. I. M. Santos, E. Oliveira, J. F. B. Barata, M. A. F. Faustino, J. A. S. Cavaleiro, M. G. P. M. S. Neves and C. Lodeiro, *Inorg. Chimica Acta,* 2013, *in press*, DOI: 10.1016/j.ica.2013.09.049.

58 L. S. H. P. Vale, J. F. B. Barata, M. G. P. M. S. Neves, M. A. F. Faustino, A. C. Tomé, A. M. S. Silva, F. A. A. Paz and J. A. S. Cavaleiro, *Tetrahedron Lett.,* 2007, **48**, 8904-8908.

59 F. D´Souza, R. Chitta, K. Ohkubo, M. Tasior, N. K. Subbaiyan, M. E. Zandler, M. K. Rogacki, D. T. Gryko and S. Fukuzumi, *J. Am. Chem. Soc.,* 2008, **130**, 14263-14272.

60 K. Lewandowska, B. Barszcz, J. Wolak, A. Graja, M. Grzybowski and D. T. Gryko, *Dyes and Pigments,* 2013, **96**, 249-255.

61 T. H. Ngo, F. Puntoriero, F. Nastasi, K. Robeyns, L. Van Meervelt, S. Campagna, W. Dehaen and W. Maes, *Chem-Eur. J.,* 2010, **16**, 5691-5705.

62 W. Maes, T. H. Ngo, J. Vanderhaeghen and W. Dehaen, *Org. Lett.,* 2007, **9**, 3165-3168.

63 A. Scrivanti, V. Beghetto, U. Matteoli, S. Antonaroli, A. Marini, F. Mandoj, R. Paolesse and B. Crociani, *Tetrahedron Lett*., 2004, **45**, 5861-5864.

64 S. Berg, K. E. Thomas, C. M. Beavers and A. Ghosh, *Inorg. Chem.*, 2012, **51**, 9911-9916.

65 M. König, L. M. Reith, U. Monkowius, G. Knör, K. Bretterbauer and W. Schöefberger, *Tetrahedron*, 2011, **67**, 4243-4252.

66 T. Kinzel, Y. Zhang and S. L. Buchwald, *J. Am. Chem. Soc.*, 2010, **132**, 14073-14075.

67 L. M. Reith, M. Koenig, C. Schwarzinger and W. Schöefberger, *Eur. J. Inorg. Chem.*, 2012, 4342-4349.

68 L. M. Reith, M. Stiftinger, U. Monkowius, G. Knör and W. Schöefberger, *Inorg. Chem.*, 2011, **50**, 6788-6797.

69 M. Bröring, M. Funk and C. Milsmann, *J. Porphyrins Phthalocyanines*, 2009, **13**, 107-113.

70 I. Nigel-Etinger, A. Mahammed and Z. Gross, *Catal. Sci. Technol.*, 2011, **1**, 578-581.

71 M. Tasior, D. T. Gryko, J. Shen, K. M. Kadish, T. Becherer, H. Langhals, B. Ventura and L. Flamigni, *J. Phys. Chem., C*, 2008, **112**, 19699-19709.

72 H.-Y. Zhan, H.-Y. Liu, J. Lu, A.-Z. Wang, L.-L. You, H. Wang, L.-N. Ji and H.-F Jiang, *J. Porphyrins Phthalocyanines*, 2010, **14**, 150-157.

73 A. G. Smith and P. B. Farmer, *Biomed. Mass Spectrom.*, 1982, **9**, 111-114.

74 J. D. Laycock, J. A. Ferguson, R. A. Yost, J. M. E. Quirke, A. Rohrer, R. Ocampo and H. Callot, *J. Mass Spectrom.*, 1997, **32**, 978-983.

75 P. Sundararaman, E. J. Gallegos, E. W. Baker, J. R. B. Slayback and M. R. Johnston, *Anal. Chem.*, 1984, **56**, 2552-2556.

76 G. J. Shaw, G. Eglinton and J. M. E. Quirke, *Anal. Chem.*, 1981, **53**, 2014-2020.

77 G. J. Van Berkel , G. L. Glish , S. A. McLuckey and A. Albert, *Anal. Chem.*, 1990, **62**, 786–793.

78 N. Evans, D. E. Games, A. H. Jackson and S. A. Matlin, *J. Chromatogr. A*, 1975, **115**, 325-333.

79 V. Sugumaran, V. Kagdiyal, R. Kumar, R. Sarin, A. K. Gupta, A. S. Sarpal and B. Basu, *Petrol. Sci. Techn.*, 2011, **30**, 278-289.

80 P. Swider, A. Nowak-Krol, R. Voloshchuk, J. P. Lewtak, D. T. Gryko and W. Danikiewicz, *J. Mass Spectrom.*, 2010, **452**, 1443-1451.

81 R. B. Freas and J. E. Campana, *Inorg. Chem.*, 1984, **23**, 4654-4658.

82 J. B. Carlson and P. Vouros, *J. Mass Spectrom.*, 1996, **31**, 1403-1408.

83 M. R. M. Domingues, M. G. O. Santana-Marques and A. J. F. Correia, *Int. J. Mass Spectrom. Ion Processes*, 1997, **165-166**, 551-559.

84 R. A. Izquierdo, C. M. Barros, M. G. O. Santana-Marques, A. J. F. Correia, A. M. G. Silva, A. C. Tomé, A. M. S. Silva, M. G. P. M. S. Neves and J. A. S. Cavaleiro, *Rapid Commun. Mass Spectrom.*, 2004, **18**, 2601-2611.

85 M. Schafer and H. Budzikiewicz, *J. Mass Spectrom.*, 2001, **36**, 1062-1068.

86 N. Srinivasan, C. A. Haney, J. S. Lindsey, W. Zhang and B. T. Chait, *J. Porphyrins Phthalocyanines*, 1999, **3**, 283-291.

87 A. Kasselouri, O. Bourdon, D. Demore, J. C. Blais, P. Prognon, G. Bourg-Heckly and J. Blais, *Photochem. Photobiol.*, 1999, **70**, 275-279.

88 H.-P. Lassalle, N. Lourette, B. Maunit, J.-F. Muller, F. Guillemin and L. Bezdetnaya-Bolotine, *J. Mass Spectrom.*, 2005, **40**, 1149-1156.

89 C. Denekamp and E. Rabkin, *J. Am. Soc. Mass Spectrom*., 2007, **18**, 791-801.

90 M. R. M. Domingues, P. Domingues, M. G. P. M. S. Neves, A. C. Tomé and J. A. S. Cavaleiro, *J. Porphyrins Phthalocyanines*, 2009, **13**, 524-527.

91 C. I. V. Ramos, M. G. O. Santana-Marques, A. J. F. Correia, V. V. Serra, J. P. C. Tomé, A. C. Tomé, M. G. P. M. S. Neves and J. A. S. Cavaleiro, *J. Am. Soc. Mass Spectrom.*, 2007, **18**, 762-768.

92 C. I. V. Ramos, M. G. O. Santana-Marques, A. J. F. Correia, J. P. C. Tomé, C. M. Alonso, A. C. Tomé, M. G. P. M. S. Neves and J. A. S. Cavaleiro, *J. Mass Spectrom.*, 2008, **43**, 806–813.

93 R. A. Izquierdo, C. M. Barros, M. G. O. Santana-Marques, A. J. F. Correia, E. M. P. Silva, F. Giuntini, M. A. F. Faustino, J. P. C. Tomé, A. C. Tomé, A. M. S. Silva, M. G. P. M. S. Neves, J. A. S. Cavaleiro, A. F. Peixoto, M. M. Pereira and A. A. C. C. Pais, *J. Am. Soc. Mass Spectrom.*, 2007, **18**, 218-225.

94 G. J. Van Berkel, S. A. McLuckey and G. L. Glish, *Anal. Chem.,*1992, **3**, 235–242.

95 V. E. Vandell and P. A. Limbach, *J. Mass Spectrom.,* 1998, **33**, 212–220.

96 I. Batinic-Haberle, R. D. Stevens, I. Fridovich, *J. Porphyrins Phthalocyanines,* 2000, **4**, 217–227.

97 J. Witowska-Jarosz, L. Gorski, E. Malinowska and M. Jarosz, *J. Mass Spectrom*., 2002, **37**, 1236–1241.

98 D. M. Tomazela, F. C. Gozzo, I. Mayer, F. M. Engelmann, K. Araki, H. E. Toma and M. N. Eberlin, *J. Mass Spectrom.*, 2004, **39**, 1161-1167.

99 K. S. F. Lau, M. Sadilek, G. E. Khalil, M. Gouterman and C. Bruckner, *J. Am. Soc. Mass Spectrom.,* 2005, **16**, 1915–1920.

100 E. M. P. Silva, C. I. V. Ramos, P, M. R. Pereira, F. Giuntini, M. A. F. Faustino, J. P. C. Tomé, A. C. Tomé, A. M. S. Silva, M. G. O. Santana-Marques, M. G. P. M. S. Neves and J. A. S. Cavaleiro, *J. Porphyrins Phthalocyanines*, 2012, **16**, 101-113.

101 C. I. V. Ramos, C. M. Barros, A. M. Fernandes, M. G. O. Santana-Marques, A. J. F. Correia, J. P. C. Tomé, M. C. T. Carrilho, M. A. F. Faustino, A. C. Tomé, M. G. P. M. S. Neves and J. A. S. Cavaleiro, *J. Mass Spectrom.*, 2005, **40**, 1439–1447.

102 C.I.V. Ramos, J.P.C. Tomé and M.G.O Santana-Marques, *J. Mass Spectrom.*, **2012**, 47, 173-179.

103 A. Rosell-Melé and J.R. Maxwell, *Rapid Commun. Mass Spectrom.*, 1996, **10**, 209-213.

104 P. Swider, J. P. Lewtak, D. T. Gryko and W. Danikiewicz, *J. Mass Spectrom*., 2013, **48**, 1116-1124.

105 D. T. Gryko, *Chem. Commun.*, 2000, **22**, 2243-2244.

106 A. E. Meier-Callahan, H. B. Gray and Z. Gross, *Inorg. Chem.*, 2000, **39**, 3605-3607.

107 T. Ding, E. A. Aleman, D. A. Modarelli, C. J. Ziegler, *J. Phys. Chem. A*, 2005, **109**, 7411-7417.

108 J. P. Collman, M. Kaplun and R. A. Decréau, *Dalton Trans.,* 2006, **4**, 554-559.

109 T. H. Ngo, W. V. Rossom, W. Dehaen and W. Maes, *Org. Biomol. Chem.*, 2009, **7**, 439-443.

110 M. Bröring, C. Milsmann, S. Ruck and S. Kohler, *J. Organometallic Chem.*, 2009, **694**, 1011-1015.

111 W. Schöfberger, F. Lengwin, L. M. Reith, M. List, G. Knör, *Inorg. Chem. Commun.*, 2010, **13**, 1187-1190.

112 S. H. Kim, H. Park, M. S. Seo, M. Kubo, T. Ogura, J. Klajn, D. T. Gryko, J. S. Valentine and W. Nam, *J. Am. Chem. Soc.*, 2010, **132**, 14030–14032.

113 M. Toganoh, Y. Kawabe and H. Furuta, *J. Org. Chem.,* 2011, **76**, 7618–7622.

114 O. G. Tsay, B.-K. Kim, T. L. Lu, J. Kwak and D. G. Churchill, *Inorg. Chem.,* 2013, **52**, 1991−1999.

115 K. S. F. Lau, M. Sadilek, M. Gouterman, G. E. Khalil and C. Bruckner, *J. Am. Soc. Mass Spectrom.,* 2006, **17**, 1306-1314.

116 C. I. V. Ramos, M. G. O. Santana-Marques, A. J. F. Correia, J. F. B. Barata, A. C. Tomé, M. G. P. M. S. Neves, J. A. S. Cavaleiro, P. E. Abreu, M. M. Pereira and A. A. C. C. Pais, *J. Mass Spectrom.*, 2012, **47**, 516-522.

117 J. B. F. Barata, C. M. Barros, M. G. O. Santana-Marques, M. G. P. M. S. Neves, M. A. F. Faustino, A. C. Tomé, A. J. F. Correia and J. A. S. Cavaleiro, *J. Mass Spectrom.*, 2007, **42**, 225-232.

118 M. Fasciotti, A. F. Gomes, F. C. Gozzo, B. A. Iglesias, G. F. Sá, R. J. Daroda, M. Toganoh, H. Furuta, K. Araki and M. N. Eberlin, *Org. Biomol. Chem.,* 2012, **10**, 8396-8402.

119 P. M. Lalli, B. A. Iglesias, D. K. Deda, H. E. Toma, G. F. Sá, R. J. Daroda, K. Araki and M. N. Eberlin, *Rapid Commun. Mass Spectrom.*, 2012, **26**, 263-268.

120 P. M. Lalli, B. A. Iglesias, H. E. Toma, G. F. Sá, R. J. Daroda, J. C. S. Filho, J. E. Szulejko, K. Araki and M. N. Eberlin, *J. Mass Spectrom.*, 2012, **47**, 712-719.

121 C. I. V. Ramos, M. G. O. Santana-Marques, R. F. Enes, A. C. Tomé, J. A. S. Cavaleiro and M. Nogueras, *J. Mass Spectrom*., 2009, **44**, 911-919.

122 A. Mahammed, J. J. Weaver, H. B. Gray, M. Abdelas and Z. Gross, *Tetrahedron Lett.,* 2003, **44**, 2077-2079.

123 L. Lvova, C. Di Natale, A. D'Amico and R. Paolesse, *J. Porphyrins Phthalocyanines*, 2009, **13**, 1168-1178.

124 A. T. Blades, M G Ikonomou and P. Kebarle, *Anal. Chem.*, 1991**, 63**, 2109-2114.

125 G. J. Van Berkel and F. Zhou, *Anal. Chem.*, 1995, **67**, 2916–2923.

126 G. J. Van Berkel in *The Electrolytic Nature of Electrospray, Electrospray Ionization Mass Spectrometry: Fundamentals, Instrumentation, and Applications*, R. B. Cole Ed., John Wiley & Sons, New York, 1997, 65-105.

127 J. F. De la Mora, G. J. Van Berkel, C. G. Enke, R. B. Cole, M. Martinez-Sanchez and J. B. Fenn, *J. Mass Spectrom.* 2000, **35***,* 939-952.

128 J. Shen, J. Shao, Z. Ou, W. E. B. Koszarna, D. T. Gryko and K. M. Kadish, *Inorg. Chem.,* 2006, **45**, 2251-2265.

129 H. Tsunematsu, H. Ikeda, H. Hanazono, M. Inagaki, R. Isobe, R. Higuchi, Y. Goto and M. Yamamoto, *J. Mass Spectrom.,* 2003, **38**, 188-195.

130 K. P. Madhusudanam, *J. Mass Spectrom.* 2006, **41**, 1096-1104.

131 H. Perreault and C. E. Costello, *J. Mass Spectrom.,* 1999, **34**, 184-197.

132 S. P. Gaucher and J. A. Leary, *Anal. Chem.,* 1998, **70**, 3009-3014.

133 X. Zhu and T. Sato, *Rapid Commun. Mass Spectrom.,* 2007, **21**, 191-198.

134 L. M. O. Lourenço, J. P. C. Tomé, M. R. M. Domingues, P. Domingues, P. J. Costa, V. Félix, M. G. P. M. S. Neves and J. A. S. Cavaleiro, *Rapid Commun. Mass Spectrom.,* 2009, **23**, 3478-3483.

135 M. R. M. Domingues, P. Domingues, A. Reis, A. J. F. Correira, J. P. C. Tomé, A. C. Tomé, M. G. P. M. S. Neves and J. A. S. Cavaleiro, *J. Mass Spectrom.*, 2004, **39**, 158-167.

136 U. Schwarz, M. Vonderach, M. Kappes, R. Kelting, K. Brendle and P. Weis, *Int. J. Mass Spectrom.*, 2013, **339-340**, 24-33.

137 A. B. Kanu, P. Dwivedi, M. Tam, L. Matz and H. H. Hill Jr., *J. Mass Spectrom.*, 2008, **43**, 1-22.

138 C. M. Benton, C. K. Lim, C. Moniz and D. J. L. Jones, *Rapid Commun. Mass Spectrom.*, 2012, **26**, 480-486.

139 L. Ahonen, M. Fasciotti, G. B. Gennäs, T. Kotiaho, R. J. Daroda, M. N. Eberlin and R. Kostiainen, *J. Chromatogr., A*, 2013, **1310**, 133-137.

140 G. R. Hilton and J. L. P. Benesch, *J. R. Soc. Interface*, 2012, **9**, 801-816.

141 M. Fasciotti, P. M. Lalli, G. Heerdt, R. A. Steffen, Y. E. Corilo, G. F. Sá, R. J. Daroda, F. A. M. Reis, N. H. Morgon, R. C. L. Pereira, M. N. Eberlin and C. F. Klitzke, *Int. J. Ion Mobil. Spec.,* 2013, **16**, 117-132.

Adventures in Corrole Features by Electrospray Ionization Mass Spectrometry Studies